



A Feasible Route to Produce 30 MPa Adhesion Strength of Electrochemically Deposited Hydroxyapatite (HA) on Titanium (Ti6Al4V) Alloy

Nosheen Maryam Awan¹ ·
Muhammad Umar Manzoor¹ · Faraz Hussain¹ ·
Zaeem Ur Rehman¹ · Muhammad Ishtiaq¹

Received: 26 September 2022 / Accepted: 5 January 2023 / Published online: 3 February 2023
© The Indian Institute of Metals - IIM 2023

Abstract Ti6Al4V alloy, an $\alpha + \beta$ titanium alloy having good biocompatibility, low density, high strength and a better resistance to corrosion is an excellent candidate for bridges and implants. Hydroxyapatite (HA), a calcium phosphate ($\text{Ca}_{10}(\text{PO}_4)_6(\text{OH})_2$) mineral having similar chemical composition with the hard tissues of human bones, was electrochemically deposited on Ti6Al4V alloy grade-5. The surface activity of substrate was increased by a uniform TiO_2 film, achieved by grinding, polishing, pretreatment with anodization and alkali treatment. Electrochemical deposition was done by HA powder-ethanol suspension with an antibacterial binder called chitosan at set parameters of 20 V for 1 h at pH 4. The adhesion ability and polarization behavior of HA-coated Ti6Al4V alloy was observed. The anodized, HA-coated, and a bare substrate alloy samples were examined in a bio-simulated solution of ringer's lactate for polarization testing. SEM and EDAX analysis were performed for HA powder and HA-deposited sample to observe the surface morphology with elemental compositions. Adhesion test (Shimadzu AGS X series tensile testing machine at 25 °C and 60% relative humidity) was performed to check the coating adhesiveness with the metallic substrate, and the observed value was upto 30 MPa. Herein, the electrochemical-deposited HA-coated samples were more resistant to dissolution and showed 2 times better corrosion resistance than bare metal. The bonding strength achieved in this work

was also 30 MPa which is greater than required for tooth fixation and root implants (20 MPa).

Keywords Hydroxyapatite · Ti6Al4V alloy · Electrochemical deposition · Anodization · Polarization

1 Introduction

Excellent biocompatibility, good strength-to-weight ratio, less weight-to-volume ratio, better corrosion resistance and superior mechanical properties of titanium and its alloys make it a suitable candidate for biomedical applications particularly in orthopedic and osteosynthesis [1–9]. The small difference of Young's modulus between human bones and some titanium alloys make them suitable implant materials as they can enhance service life by minimizing the stress shielding effect [7, 10, 11]. Although the ability of titanium to form a TiO_2 layer makes it corrosion-resistant but this layer has poor mechanical strength and can lead to failure of the implant at extreme conditions [12–16]. Surface modification for better metallic implant fixation with natural bone is inevitable otherwise, leaching of Al and V can result in diseases like osteomalacia, alzheimer and neuropathy by exceeding the threshold limit [17, 18]. Surface modifications of bioimplants is done by various methods like, chemical [19, 20], physical [21], electrochemical [22], thermal [23], plasma spray [24], sol-gel [25] and ion implantation [26].

Body implants can be coated with a bioactive calcium phosphate ceramic material known as hydroxyapatite (HA) with chemical formula of $\text{Ca}_{10}(\text{PO}_4)_6(\text{OH})_2$ to get a better strength to avoid failure at extreme conditions [27–31]. It is a naturally occurring mineral and is also found in different human body parts e.g. bones, brain and teeth enamels [32–34]. It has brightened the medical field because of its better chemical

✉ Nosheen Maryam Awan
nosheen.mme@pu.edu.pk

✉ Muhammad Ishtiaq
ishtiaq.imme@pu.edu.pk

¹ Institute of Metallurgy and Materials Engineering, Faculty of Chemical and Materials Engineering, University of the Punjab, Lahore, Pakistan

bonding and is being used in surgeries of bones, teeth, hip, knee joints, filling cavities, repairing damaged parts and many others. HA has also found its applications as coating material for medical and prosthetic devices [35]. Enormous attention has been paid to HA coatings on metallic implants because it can overcome some serious issues like brittleness, release of V, Al ions [28–30, 36–41].

Electrochemical deposition technique is easy to use at its low working temperature with varying current and voltage parameters [42]. The composition of phase and coating morphology of hydrothermally electrochemically deposited HA-TiO₂ coating on Ti6Al4V was previously studied, and it was concluded that these were significantly affected by anodizing voltages [43]. A maximum of 19 MPa adhesion strength was obtained by applying fluoridated HA coatings [44]. CVD technique used by some researchers to deposit graphene-based carbon–carbon composites coating with HA reported a bonding strength of only 12.56 MPa [45]. Surface morphology is the main factor upon which the properties of dental implants are dependent. The literature reveals the advantages and disadvantages of surface modifications [46–49]. A few attempts by using additional materials like zirconia [50], titania [51–53], caprolactone [54], calcium silicate [55], few other [40, 56–59] have already been done to enhance the bonding strengths of HA coatings. None of the previous studies have developed HA coating having more than 21 MPa adhesion strength according to best of our knowledge.

Using a simple and easily approachable technique like electrochemical deposition to get best possible adhesion strength is need of the hour. This study was carried out to develop HA coating on Ti6Al4V by electrochemical deposition technique to get adhesion strength more than the earlier reported ones.

2 Experimental Details

2.1 Sample Preparation

The chemical composition (wt.%) Ti6Al4V alloy used as substrate is given in Table 1.

Samples with 10 mm × 10 mm × 2 mm were cut, ground with SiC papers and polished with diamond paste. The polished samples were cleaned with ethanol and distilled water. The samples were then dipped in methanol in sonication bath for 10 min and were placed in a desiccator after drying.

Table 1 Chemical composition (wt%) of Ti6Al4V alloy

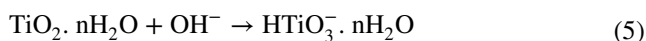
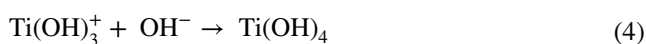
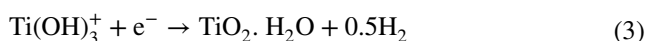
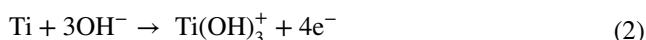
Titanium alloy	Chemical composition				
Ti6Al4V	Al	Mo	V	Fe	Ti
	6	0.002	4	0.003	Balance

2.2 Anodization of the Sample

The samples were anodized in a 1 M solution of H₂SO₄ with slow magnetic stirring for maintaining homogeneity of the solution for 10 min at 30 V. A graphite electrode was used as anode, whereas the mechanically prepared substrate sample was considered as cathode. Samples were cleaned in distilled water and ethyl alcohol after anodization. A porous TiO₂ layer was deposited over Ti6Al4V substrate to increase the bioactivity.

2.3 Alkali Treatment

After anodization, the surface of Ti6Al4V samples were treated by 5 M NaOH alkali solution to form a thin sodium titanate layer on the surface as done by some previous researchers [60–62]. The main purpose of this alkali treatment was to induce apatite formation by forming a sodium titanate layer. This formation was facilitated by surface functional sites consisting of Ti–OH groups [63, 64]. TiO₂ layer formed during anodization reacts with hydroxyl group in alkali solution as given in below equations:



The samples were heated in this solution for 15 min at 60 °C at a hot plate to increase the rate of calcium phosphate nucleation. The samples were then washed in ultrasonic bath for 10 min and dried in hot air.

2.4 Hydroxyapatite Suspension Solution

The suspension solution was prepared by adding of 1.2 gm of HA powder in 50 ml of ethyl alcohol, the adjustment of pH was made by the addition of few drops of HCl/HNO₃ acid for keeping its value at a level of 4. The suspension was sonicated in ultrasonication bath for 30 min for HA dispersion in the solution.

2.5 Electrochemical Deposition

The pretreated sample was connected to the cathodic terminal and graphite electrode to the anodic terminal at 20 V for 1 h with slow magnetic stirring of suspension

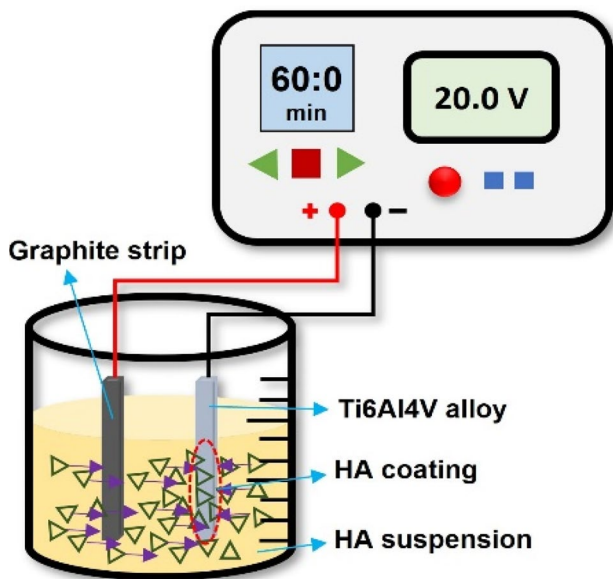


Fig. 1 Schematic representation of HA coating on Ti6Al4V alloy

solution (Fig. 1). During this process, hydrogen evolution on cathode could occur which was prohibited by adding H_2O_2 in the solution, which in return promoted nucleation rate and growth of HA coating [65]. The coated samples were then heat treated at $50\text{ }^\circ\text{C}$ on a hot plate for 15 min followed by aircooling to room temperature. These heat treated samples were then placed in a desiccator. This heat treatment results in near perfect bonding of the implant with living bones [60, 66].

2.6 Chitosan Solution

Chitosan (0.5 g/l), having anti-bacterial properties [36], was added in 1% acetic acid and sonicated for 10–15 min for homogeneous gel solution formation. This chitosan gel solution was painted on heated HA-coated samples and allowed to dry.

2.7 Scanning Electron Microscopy

Scanning electron microscope (SEM) (Inpect-S50, Thermo Fisher Scientific, USA) was used to study the surface characteristics of HA-coated Ti6Al4V alloy. EDX elemental analysis at an accelerating voltage of 15 kV was also performed to find Ca, P and O present in the coating and HA powder. These are the required constituents for the natural bone configuration as used in the form of HA powder.

2.8 Electrochemical Testing

A potentiostat/galvanostat (GAMRY instruments, USA, reference 3000) was used for electrochemical testing. Ringer's

lactate solution was used as electrolyte, saturated calomel electrode (SCE) as a standard electrode, selected sample as a working electrode and graphite as a counter electrode. Tafel scan was drawn at a potential range of -0.5 to $+0.5$ V with scan rate of 3 mV/s with 1 cm^2 sample selected area. (Gram equivalent weight is 23.933.)

2.9 Adhesion Testing

The adhesion testing of coated samples were performed at Universal force testing machine (Chatillon LCTM-500) with 2.5 kN load cell, 5 mm/min crosshead speed, at room temperature ($25\text{ }^\circ\text{C}$) and 60% relative humidity in accordance with ISO 13779-4:2002(E).

3 Results and Discussion

3.1 SEM and EDX Analysis

SEM micrographs shown in Fig. 2 are depicting that the HA particles are effectively deposited on Ti6Al4V alloy substrate using an electrochemical coating process. A good adhesion between HA particles and substrate is achieved. On the substrate surface, there is no significant delamination of the coating, indicating that the HA suspension solution is uniformly deposited. SEM images are clearly showing the uniformity and uncracking of coating.

EDX spectroscopy with quantitative analysis presenting the weight percent of Ca, P and O of spot 1 HA-deposited Ti6Al4V alloy is shown in Fig. 3.

Here, the Ca/P ratio in spot 1 is 3.029 by weight percent, and the molar ratio ($0.0111/0.004729 = 2:35$) is (wt. of Ca/40)/(wt. of P/31). The bioactivity of the implant increases as the ratio rises. The formability of $CaTiO_3$ directly producing HA in the coating will increase as the Ca/P ratio in the electrolyte increases [67]. The low percentage of Ca and P in the coating indicates that it may be thin at times.

Figure 4 shows the results of HA powder analysis using SEM at various micron levels in order to see the nano-sized particles. The shape and size of a substance have a significant impact on its bioactivity and can increase its bioactive qualities [68]. The particles of irregular shapes are observed in the agglomerated form. At higher magnification, particles are agglomerated forming the grains of large dimensions, in other words, large grains are formed from small particle agglomeration.

SEM micrographs of HA powder are shown in Fig. 5 with three spots at different positions, each with its unique spectra and quantitative findings. These spots were captured at three separate points to show the weightage of major elements, while Fig. 6 demonstrates the mean value of these elements at these three spots. The small difference in mechanical properties, e.g., fracture toughness of implants and natural

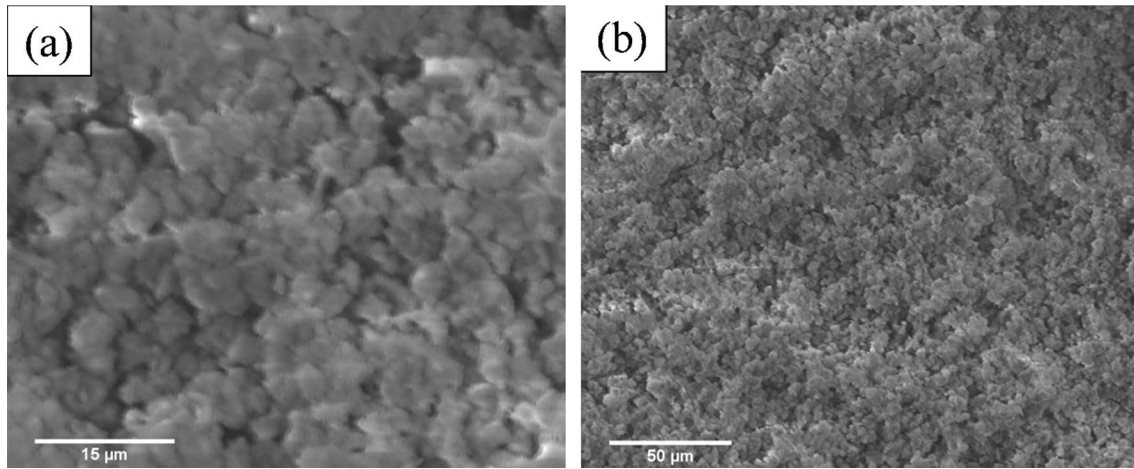


Fig. 2 SEM micrographs of uncrack deposition surface **a** HA deposited Ti6Al4V alloy at 5000X, **b** HA deposited Ti6Al4V alloy at 1000X

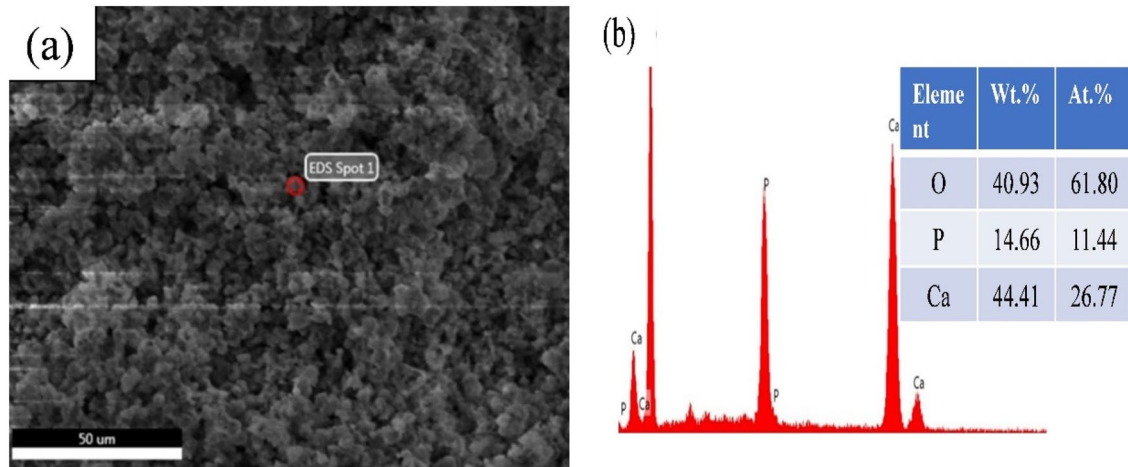


Fig. 3 EDX spectrum of HA deposited Ti6Al4V alloy **a** SEM surface micrograph and **b** EDS spot analysis with quantitative results of HA deposited sample

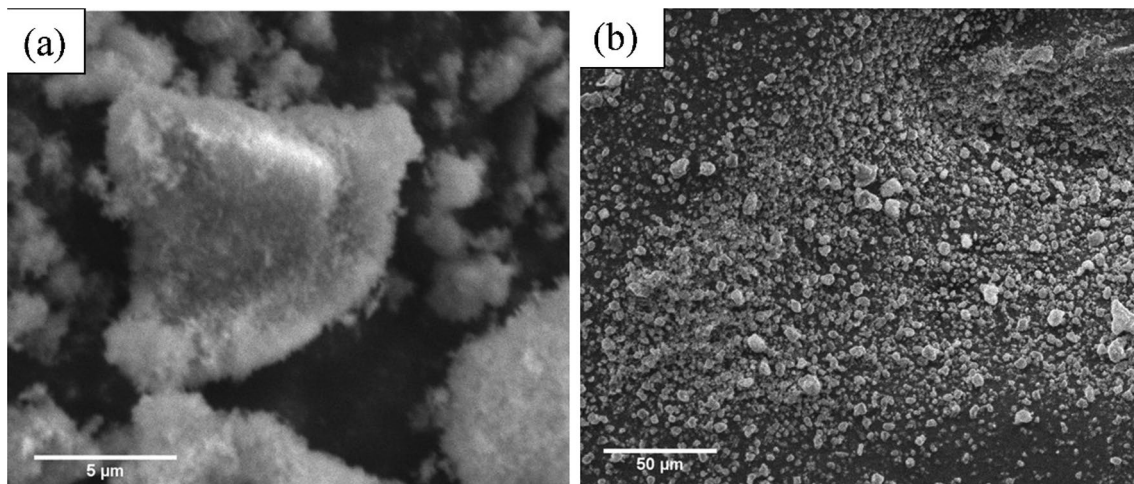


Fig. 4 HA powder SEM micrographs at different micron level

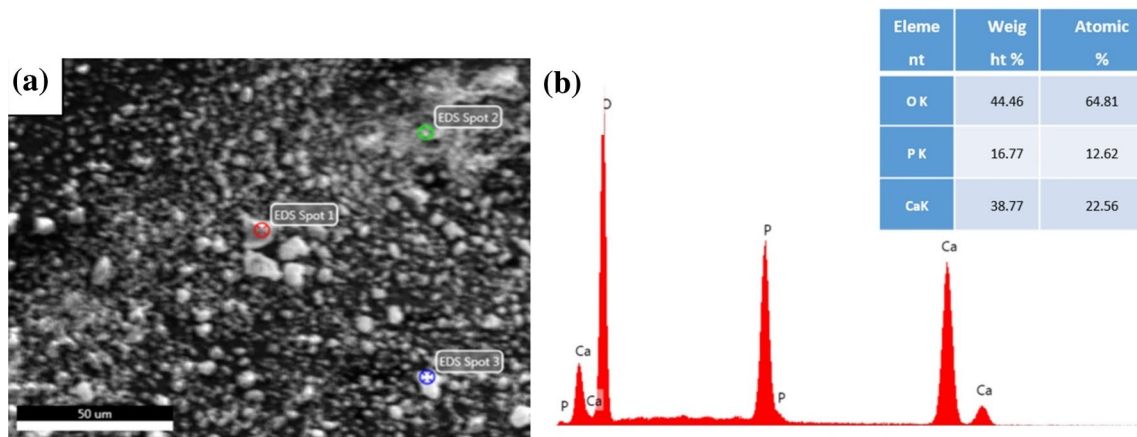


Fig. 5 a SEM micrograph at 2000X, b EDX spectrum of spot 1 and its quantitative results

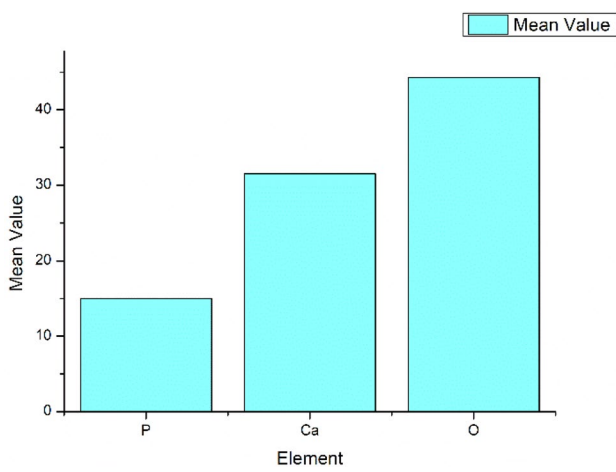


Fig. 6 EDX spot analysis of HA powder at three spots with their descriptive statistics

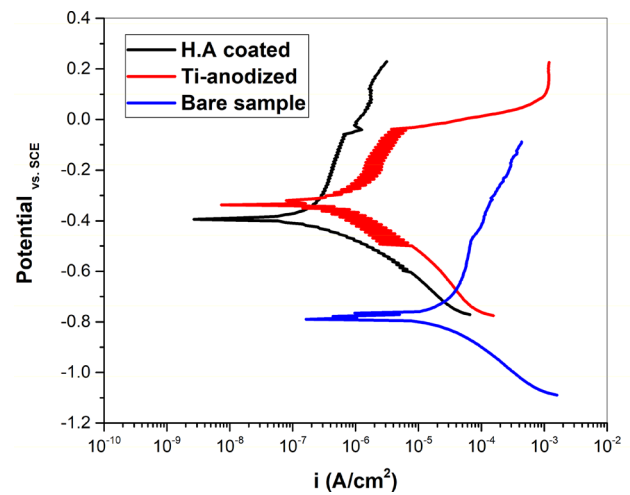


Fig. 7 Polarization curves of all HA coated, Ti-anodized and bare Ti6Al4V alloy with scan rate of 3 mV/s

bones, can be further minimized by thin coatings, and these thin coatings will have a negligible effect on human cells, proteins and molecules as reported previously [69]. As a result, rather than thick coatings those can cause delamination and implant failures, we can accomplish superior osteointegration in tissues with stable development. According to studies, the carbonate containing apatite coating on a bio-material is the primary need in order to get an optimum bonding with the living bones [70, 71].

3.2 Electrochemical Testing

The polarization curves of HA-coated, Ti-anodized and bare samples (grinded and polished Ti6Al4V) are shown in Fig. 7.

The polarization curves for anodized and coated samples showing low corrosion rate as compared to bare/uncoated sample. Polarization rate between coated and anodized alloy substrate showing a close relationship, as anodization, was

used to boost the surface activity for HA coating in sulfuric acid, which resulted in the formation of a TiO₂ layer, a ceramic layer that aids in the reduction in corrosion rates.

The curve for bare sample has moved toward more active side confirming more oxidation as shown in Fig. 7, whereas, the curve for HA-coated Ti6Al4V is toward less active (positive) side confirming the formation of a passive protective layer.

The values of I_{corr} , E_{corr} and corrosion rate were calculated and are shown in the Table 2.

The corrosion rate of HA coated Ti6Al4V is the least among all three samples as shown in Table 2. The corrosion rate has dropped from 2.3010 mpy (bare Ti6Al4V) to 0.0469 mpy (HA-coated Ti6Al4V). The formation of TiO₂ layer, a ceramic layer in Ti-anodized sample, aids in the reduction in corrosion rate. The composition and concentration of the electrolyte utilized determine the dissolving properties of the oxide coating. The resistance ability of the HA-coated

sample is better than that of anodized titanium alloy. R_p is a corrosion resistant factor, which implies that if its value is high, the rate of corrosion is lower and the materials have superior corrosion resistance. R_p values also confirm the highest corrosion resistance of HA-coated Ti6Al4V alloy in body simulated fluid/solution. R_p is determined using these slopes (ASTM Standard G3-89) in the equation form [37].

$$R_p = \frac{\beta_a \beta_c}{2.303 I_{corr} (\beta_a + \beta_c)}$$

Here, a and c are the anodic and cathodic Tafel slopes, respectively.

The HA layer acts as a barrier to the transit of ions and electrons between the substrate and the electrolyte, slowing down the reaction rate.

3.3 Adhesion Testing

For the evaluation of bonding or adhesive strength of HA-coated Ti6Al4V alloy, a test for different periods of time 2, 4, 6 h was performed using a preload of 2.5 kN at a load rate of 5 mm/min following the previously reported values [72]. The anodization of Ti6Al4V alloy substrate helps in the deposition of HA on the substrate which increases strength. A reasonable increase in

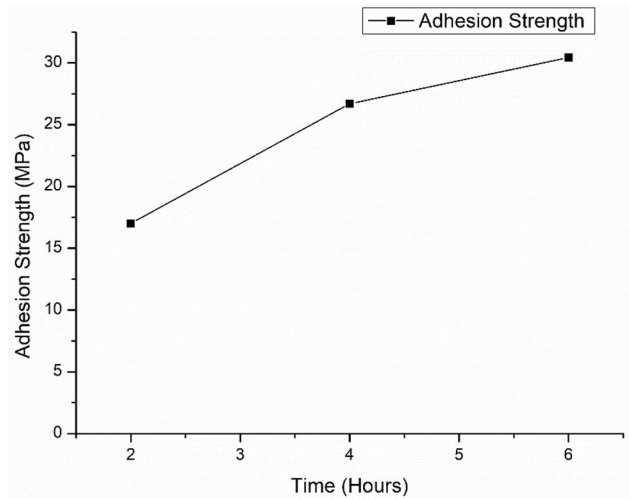


Fig. 8 Adhesive strength of anodized HA coated Ti6Al4V alloy

adhesion strength is observed, and maximum strength is 30.432 MPa and minimum 17.008 MPa as shown in Fig. 8. The minimum adhesion strength (17.008 MPa) obtained is still higher than the minimum requirement (15 MPa) for surgical applications [73]. Chitosan adds stability and increases the adhesion strength, wear

Table 2 The corrosion rate calculated from potentiodynamic polarization curves corresponding to the untreated and treated Ti6Al4V alloy surfaces

Sample	β_a (v/decade)	β_c (v/decade)	I_{corr} (A/cm ²)	E_{corr} (mV)	R_p (K Ω cm ²)	Corrosion rate (mpy)
Bare Ti6Al4V	48.00 e ⁻³	29.90 e ⁻³	3.360 e ⁻⁶	-784.0	2.38 e ³	2.3010
Ti-anodized	71.00 e ⁻³	39.00 e ⁻³	197.0 e ⁻⁹	-329.0	5.55 e ⁴	0.1350
HA coated	79.90 e ⁻³	47.30 e ⁻³	68.50 e ⁻⁹	-392.0	1.88 e ⁵	0.0469

Table 3 Adhesion strength of HA coatings deposited by different researchers

Sr. No	Composition	Adhesion strength (MPa)	References
1	CoCrMo + HAp	17.5	[76]
2	Ti6Al4V + spherical HAp (sHAp)	10.7	[72]
3	Ti6Al4V + flake-shaped HAp (fHAp)	6.8	[72]
4	Ti6Al4V + needle-shaped HAp (nHAp)	8.5	[72]
5	Ti6Al4V + sHAp/ CNT-Ti	10.6	[72]
6	Ti + HAp	15.3	[77]
7	Ti + HAp without oxidation	5	[78]
8	Ti + HAp with oxidation	7.3	[78]
9	Ti6Al4V + HAp	13.8	[79]
10	Ti6Al4V + TiO ₂ (50 V) + HAp	11.9	[79]
11	Ti6Al4V + TiO ₂ (20 V) + HAp	13.1	[79]
12	Ti6Al4V + TiO ₂ (10 V) + HAp	21	[79]
13*	Ti6Al4V + TiO ₂ (20 V) HAp	30.432*	*Our result

resistance and proliferation with antibacterial activity, which in turn increases the implant life [74].

The excellent adhesion between Ti6Al4V and HA coating was provided by TiO₂ interfacial bonding [75]. Adhesion strength of 30.432 MPa obtained in our study is the highest reported till now as can be seen from Table 3 which proves the uniqueness and novelty of our research work.

4 Conclusions

In conclusion, among various coating techniques, electrochemical coating deposition technique can be applied to get optimum adhesion strength. A maximum of 30.432 MPa adhesion strength was achieved by HA coating on Ti6Al4V substrate at 20 V. HA-coated Ti6Al4V sample provided a better protection barrier than uncoated sample. The adhesion strength reported in this work is the highest till now.

Declarations

Conflict of interest The authors report that there is no competing interest to declare.

References

- Brown S A and J E Lemons. *Medical Applications of Titanium and Its Alloys: The Material and Biological Issues* (1996).
- Williams D F. *Biocompatibility of Clinical Implant Mtls.* CRC-Press (1981).
- Long M, and Rack H J, *Biomaterials* **19** (1998) 1621.
- Fonseca C, and Barbosa M A, *Corros Sci* **43** (2001) 547.
- Chen Q, and Thouas G A, *Mater Sci Eng R Rep* **87** (2015) 1.
- Geetha M, Singh A K, Asokamani R, and Gogia A K *Prog Mater Sci* **54** (2009) 397
- Gepreel MA-H, and Niinomi M, *J Mech Behav Biomed Mater* **20** (2013) 407.
- Manivasagam G, Dhinasekaran D, and Rajamanickam A, *Recent Patents Corros Sci* **2** (2010) 1.
- Taddei E B, Henriques V A R, Silva C R M, and Cairo C A A, *Mater Sci Eng C* **24** (2004) 683.
- Nasab M B, Hassan M R, and Sahari B B, *Trends Biomater Artif Organs* **24** (2010) 69.
- Patel N R, and Gohil P P, *Int J Emerg Technol Adv Eng* **2** (2012) 91.
- Mu Y, Kobayashi T, Tsuji K, Sumita M, and Hanawa T, *J Mater Sci Mater Med* **13** (2002) 583.
- Thull, R. and M. Schaldach, *Corrosion of highly stressed orthopedic joint replacements*, in *Engineering in medicine*. 1976, Springer. p. 242-256.
- Hoepfner D W, and Chandrasekaran V, *Wear* **173** (1994) 189.
- Rabbe L M, Rieu J, Lopez A, and Combrade P, *Clin Mater* **15** (1994) 221.
- Thull R and Schaldach M, *Corrosion of Highly Stressed Orthopedic Joint Replacements*, in *Engineering in Medicine: Volume 2: Advances in Artificial Hip and Knee Joint Technology*, M. Schaldach and D. Hohmann, Editors. 1976, Springer: Berlin, Heidelberg. p. 242–256.
- Rao S, Ushida T, Tateishi T, Okazaki Y, and Asao S, *Bio-Med Mater Eng* **6** (1996) 79.
- Yumoto S, Ohashi H, Nagai H, Kakimi S, Ogawa Y, Iwata Y, Ishii K, et al., *Int J PIXE* **2** (1992) 493.
- Wen H B, Wolke J G C, de Wijn J R, Liu Q, Cui F Z, and de Groot K, *Biomaterials* **18** (1997) 1471.
- P Andrezza, M.I De Barros, C Andrezza-Vignolle, D Rats, L Vandenbulcke (1998) *Thin Solid Films*. **319**: 62.
- Uchida M, Nihira N, Mitsuo A, Toyoda K, Kubota K, and Aizawa T, *Surf Coat Technol* **177178** (2004) 627.
- X Nie, E.I Meletis, J.C Jiang, A Leyland, A.L Yerokhin, A Matthews (2002) *Surf Coat Technol* **149**: 245.
- Gülyüz H, and Çimenoglu H, *Biomaterials* **25** (2004) 3325.
- Kweh S W K, Khor K A, and Cheang P, *Biomaterials* **23** (2002) 775.
- Brendel T, Engel A, and Rüssel C, *J Mater Sci Mater Med* **3** (1992) 175.
- Hanawa T, Kamiura Y, Yamamoto S, Kohgo T, Amemiya A, Ukai H, Murakami K, and Asaoka K, *J Biomed Mater Res* **36** (1997) 131.
- Sathishkumar S, Louis K, IShinyjoy E, Gopi (2016) *Industrial & Engineering Chemistry Research* **55**: 6331.
- Chai C, and Ben-Nissan B, *J Mater Sci Mater Med* **10** (1999) 465.
- D'Antonio J A, Capello W N, Manley M T, Geesink R G T, and Jaffe W L, Hydroxyapatite femoral stems for total hip arthroplasty: 10–14 year follow-up. in *Fifteen Years of Clinical Experience with Hydroxyapatite Coatings in Joint Arthroplasty*, Springer (2004), pp 235–241.
- Gross K A, Chai C S, Kannangara G S, Ben-Nissan B, and Hanley L, *J Mater Sci Mater Med* **9** (1998) 839.
- Mediaswanti K, Wen C, Ivanova E P, Berndt C C, and Wang J, *Titanium Alloys Adv Propert Control* **21** (2013) 23.
- Fernández-Pradas J M, Clèries L, Martínez E, Sardin G, Esteve J, and Morenza J L, *Biomaterials* **22** (2001) 2171.
- Guo L, and Li H, *Surf Coat Technol* **185** (2004) 268.
- Liu D, Savino K, and Yates M Z, *Surf Coat Technol* **205** (2011) 3975.
- Song Y, Shan D, and Han E, *Mater Lett* **62** (2008) 3276.
- Ramakrishna S, Mayer J, Wintermantel E, and Leong K W, *Compos Sci Technol* **61** (2001) 1189.
- Sridhar T, Mudali U K, and Subbaiyan M, *Corros Sci* **45** (2003) 2337.
- Staiger M P, Pietak A M, Huadmai J, and Dias G, *Biomaterials* **27** (2006) 1728.
- Zhong Z, Qin J, and Ma J, *Mater Sci Eng C* **49** (2015) 251.
- Yang Y, Kim K-H, and Ong J L, *Biomaterials* **26** (2005) 327.
- Asri R I M, Harun W S W, Hassan M A, Ghani S A C, and Buoyong Z, *J Mech Behav Biomed Mater* **57** (2016) 95.
- He D, Wang P, Liu P, Liu X, Ma F, Li W, Chen X, Zhao J and Ye H, *J Wuhan Univ Technol Mater Sci Ed* **31** (2016) 461.
- Zhang S, Wang Y S, Zeng X T, Khor K A, Weng W, and Sun D E, *Thin Solid Films* **516** (2008) 5162.
- Guan K, Zhang L, Zhu F, Li H, Sheng H, and Guo Y, *J Alloys Compd* **821** (2020) 153543
- Martin J Y, Schwartz Z, Hummert T W, Schraub D M, Simpson J, Lankford J, Dean D D, Cochran D L, and Boyan B D, *J Biomed Mater Res* **29** (1995) 389.
- Schwartz Z, Martin JY, Dean DD, Simpson J, Cochran DL and Boyan BD, *Journal of Biomedical Materials Research: An Official Journal of The Society for Biomaterials and The Japanese Society for Biomaterials* **30** (1996) 145.
- Chehroudi B, McDonnell D, and Brunette D, *J Biomed Mater Res Off J Soc Biomater Jpn Soc Biomater* **34** (1997) 279.
- Brunette D, *Int J Oral Maxillofac Implants* **3** (1988) 4.

49. Qiu D, Wang A, and Yin Y, *Appl Surf Sci* **257** (2010) 1774.
50. Catauro M, Papale F, and Bollino F, *J Non-Crystal Solids* **415** (2015) 9.
51. Farrokhi-Rad M, Khosrowshahi Y B, Hassannejad H, Nouri A, and Hosseini M, *Mater Res Express* **5** (2018) 115004
52. Qiu D, Yang L, Yin Y, and Wang A, *Surf Coat Technol* **205** (2011) 3280.
53. Yusoff M F M, Rafiq M, Kadir A, Iqbal N, Hassan, M A, and Hussain R, *Surf Coat Technol* **245** (2014) 102.
54. Huang Y, Han S, Pang X, Ding Q, and Yan Y, *Appl Surf Sci* **271** (2013) 299.
55. Zhong Z, Qin J, and Ma J, *Ceram Int* **41** (2015) 8878.
56. Zhang X, Li Q, Li L, Zhang P, Wang Z, and Chen F, *Mater Lett* **88** (2012) 76.
57. Vahabzadeh S, Roy M, Bandyopadhyay A, and Bose S, *Acta Biomater* **17** (2015) 47.
58. Janković A, Eraković S, Vukašinović-Sekulić M, Mišković-Stanković V, Park S J, and Rhee K Y, *Prog Organ Coat* **83** (2015) 1.
59. Kokubo T, and Yamaguchi S, *Open Biomed Eng J* **9** (2015) 29. <https://doi.org/10.2174/1874120701509010029>
60. Ravelingien M, Mullens S, Luyten J, Meynen V, Vinck E, Vervaeet C and Remon JP, *Ceramics-Silikaty* **54** (2010) 3.
61. Suzan B, Saber Y, Maximilian M, Edward V, and Amir Z, *Materials* **8** (2015) 1612.
62. Takadama H, Kim HM, Kokubo T and Nakamura T, *J Biomed Mater Res Off J Soc Biomater Jpn Soc Biomater Aust Soc Biomater Korean Soc Biomater* **57** (2001) 441.
63. Ravelingien M, Mullens S, Luyten J, Meynen V, Vinck E, Vervaeet C, and Remon J P, *Appl Surf Sci* **255** (2009) 9539.
64. Harun W S W, Asri R I M, Alias J, Zulkifli F H, Kadirgama K, Ghani S A C, and Shariffuddin J H M, *Ceram Int* **44** (2018) 1250.
65. Kokubo T, and Yamaguchi S, *Open Biomed Eng J* **9** (2015) 29.
66. Kim H-M, Miyaji F, Kokubo T, and Nakamura T, *J Biomed Mater Res* **32** (1996) 409.
67. Yang Z, Xia L, Li W and Han J, *J Adv Biomed Eng Technol* **2** (2015) 13.
68. Williams D F, *Bioactive Mater* **10** (2022) 306.
69. Zhu L, Luo D, and Liu Y, *Int J Oral Sci* **12** (2020) 1.
70. Woesz A, and Best S, Cellular response to bioceramics. in *Cellular Response to Biomaterials*, Elsevier (2009), pp 136–155.
71. Ducheyne P, *J Biomed Mater Res* **21** (1987) 219.
72. Kwok C T, Wong P K, Cheng F T, and Man H C, *Appl Surf Sci* **255** (2009) 6736.
73. STANDARD, I., *Implants for surgery-hydroxyapatite* (2008).
74. Avcu E, Baştan F E, Abdullah H Z, Ur Rehman M A, Avcu, Y Y, and Boccaccini A R, *Prog Mater Sci* **103** (2019) 69.
75. Nie X, Leyland A, and Matthews A, *Surf Coat Technol* **125** (2000) 407.
76. Wang L-N, and Luo J-L, *Mater Charact* **62** (2011) 1076.
77. Pei X, Zeng Y, He R, Li Z, Tian L, Wang J, Wan Q, Li X, and Bao H, *Appl Surf Sci* **295** (2014) 71.
78. Zhang Y-y, Tao J, Pang Y-c, Wang W, and W Tao, *Trans Nonferrous Met Soc China* **16** (2006) 633.
79. Albayrak O, El-Atwani O, and Altintas S, *Surf Coat Technol* **202** (2008) 2482.

Publisher's Note Springer Nature remains neutral with regard to jurisdictional claims in published maps and institutional affiliations.

Springer Nature or its licensor (e.g. a society or other partner) holds exclusive rights to this article under a publishing agreement with the author(s) or other rightsholder(s); author self-archiving of the accepted manuscript version of this article is solely governed by the terms of such publishing agreement and applicable law.